Charm Jet Tagging in Charged-Current Interactions at EIC: Detector Modeling, Jet Tagging, and Intrinsic Strangeness

Stephen Sekula[1] Miguel Arratia[2] Yulia Furletova[3] Tim Hobbs[1,4] Olek Kusina[5]
Pavel Nadolsky[1] Fred Olness[1]

[1]Southern Methodist University, Dallas, TX; [2]University of California, Riverside, Riverside, CA; [3]Thomas Jefferson National Accelerator Laboratory, Newport News, VA; [4]EIC Center at Jefferson Lab, Newport News, VA; [5]Institute of Nuclear Physics PAN, Krakow, Poland

May 21, 2020

Outline

Baseline EIC Detector Implementation in Delphes

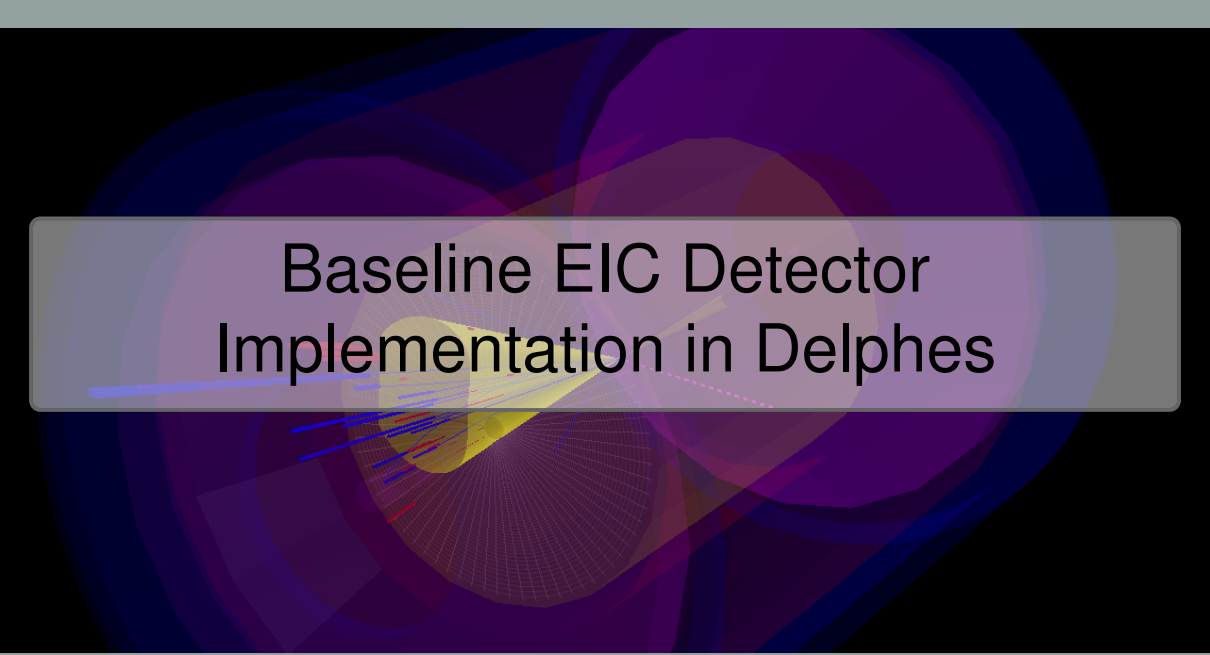

Collider Configuration[6] and Physics Goals

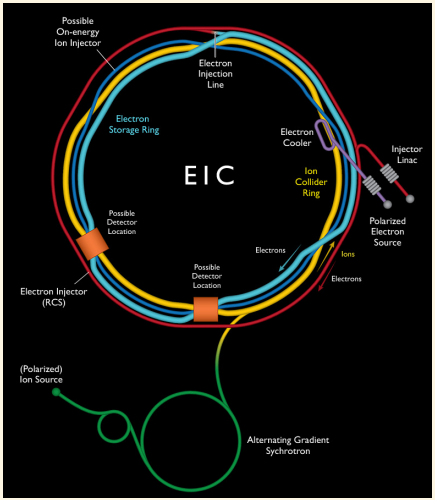

Image from Ref. [1]

The electron-hadron beam model employed for the studies shown here is an e^- and p^+ collision with $E_e = 10\ \mathrm{GeV}$ and $E_p = 275\ \mathrm{GeV}$. This achieves $\sqrt{s} \approx 105\ \mathrm{GeV}$, high instantaneous luminosity, and can yield $\approx 100\,\mathrm{fb}^{-1}$/year [2, 3].

Physics Goals

- Study **intrinsic strange and charm in the proton/nucleus** $\rightarrow$ improve understanding of strange PDF and helicity.
- Model EIC and baseline detector and observe how choices (e.g. PDFs, detector components) affect sensitivity to this physics
- Utilize jet production at EIC and jet flavor identification as platform for investigation
- We want to acknowledge existing work on charm tagging [4] by Ernst Sichtermann and Yue-Shi Lai (LBNL) using GEANT3, a silicon tracker concept, and signed, ordered track impact parameter significance (c.f. Ref. [5]).

Delphes and Detector Implementation[6]

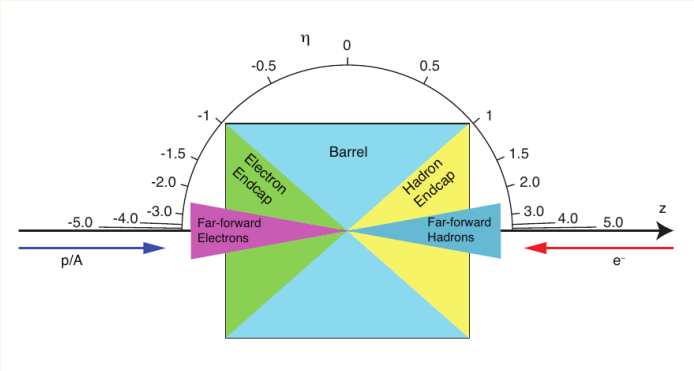

Utilizing Delphes detector implementation [7][8] based on EIC Detector Matrix [9]. See Appendix slides 29-30 for detailed breakdown.

- Tracking: covers $|\eta| < 3.5$ with 85%-98% efficiency depending on p_T and η; track impact parameter resolution is $20\mu\mathrm{m}$ is d_0 and z_0. Tracking system immersed in 1.5T magnetic field.
- ECal covers $|\eta| < 4$ with resolution of $\sigma = E \times (1.0\%) \oplus \sqrt{E} \times (2.0\%)$ in the backward direction worsening to $E \times (2.0\%) \oplus \sqrt{E} \times (12.0\%)$ in the forward direction. Granularity is $(\Delta\eta, \Delta\phi) = (0.020, 0.020)$.
- HCal covers $|\eta| < 4$ with resolution of $\sigma = E \times (10\%) \oplus \sqrt{E} \times (50\%)$ in the backward and forward direction, worsening to $E \times (10.0\%) \oplus \sqrt{E} \times (100\%)$ in the barrel. Granularity is best in forward/backward region, $(\Delta\eta, \Delta\phi) = (0.025, 0.025)$, and more coarse in the barrel, $(\Delta\eta, \Delta\phi) = (0.1, 0.1)$

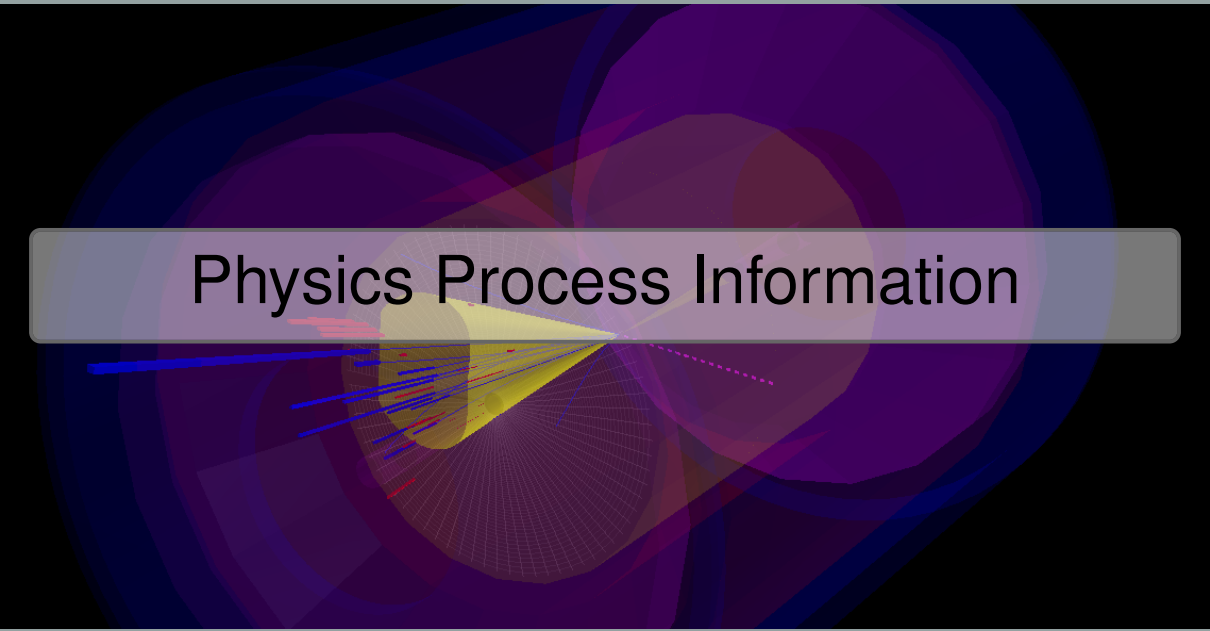

Physics Process Information

Physics Process of Interest - Charged-Current Scattering

- Charged-Current (CC) DIS is simulated using PYTHIA8 [10, 11]
  - Process: `WeakBosonExchange:ff2ff(t:W)`
  - $Q^2 > 100\ \mathrm{GeV}^2$
  - $\sigma^{PYTHIA8}_{Q^2>100\ \mathrm{GeV}^2} = 14.76\,\mathrm{pb}$
- PDF set: CT18 from LHAPDF; baseline is CT18NNLO
- Generated 10M events for study (using varying amounts of this for the parts of this talk)

Feynman Diagram for CC DIS

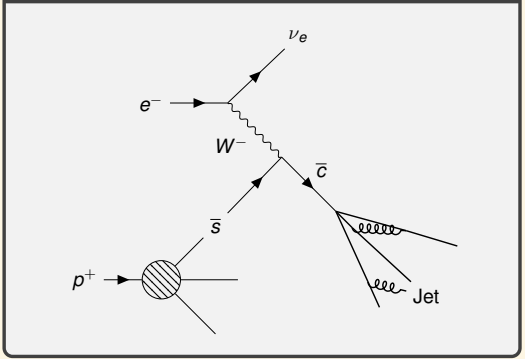

Differential Cross Sections and Yields for 100fb^{-1}

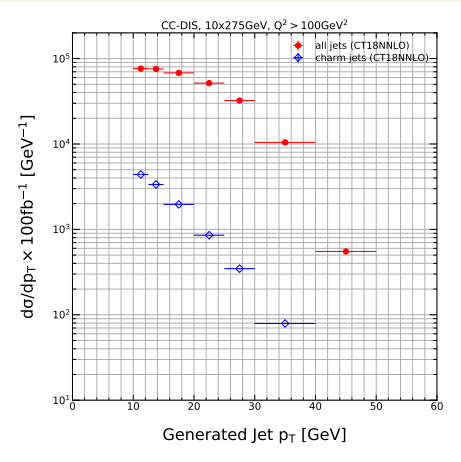

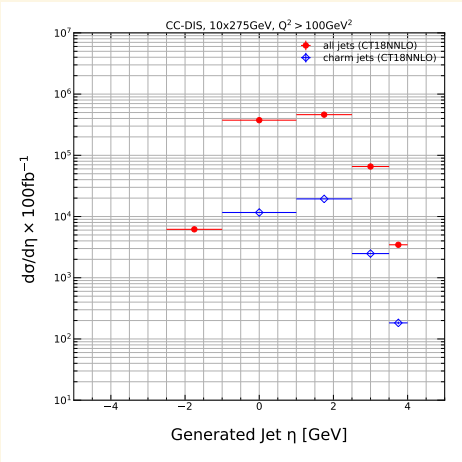

PYTHIA8 + CT18(A)N(N)LO PDFs lead to expectation of thousands of charm jets produced in 100fb^{-1} from CC DIS.

Validation Plots for Reconstructed Jets (R=1.0)

Jets are reconstructed using tracks and calorimeter clusters in an EnergyFlow approach. The Anti-k_T algorithm builds the jet (R=1.0) and energy flow is used to recompute the jet four-vector. The reconstruction implementation comes from FastJet [12, 13].

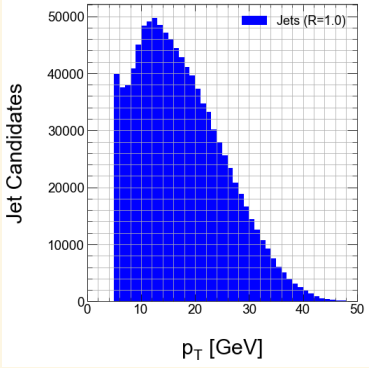

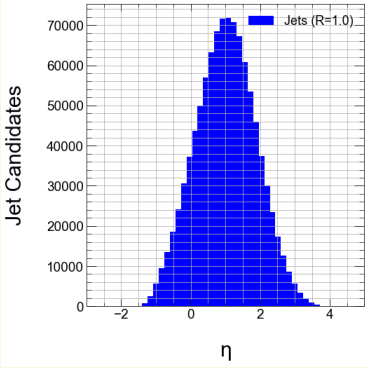

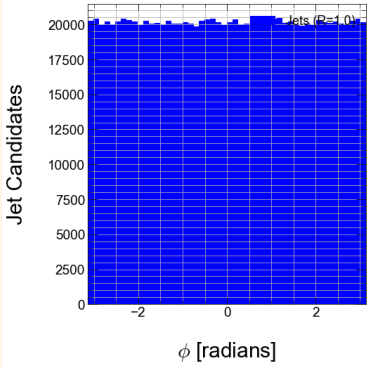

Jets well-contained in the barrel tracking volume will have $|\eta| < 1.0$, given the radius parameter of these jets; those well-contained in the forward/backward regions of the tracker will have $|\eta| = [1.5, 3.0)$. See Appendix slide 32 for resolution modeling (summary: no big surprises).

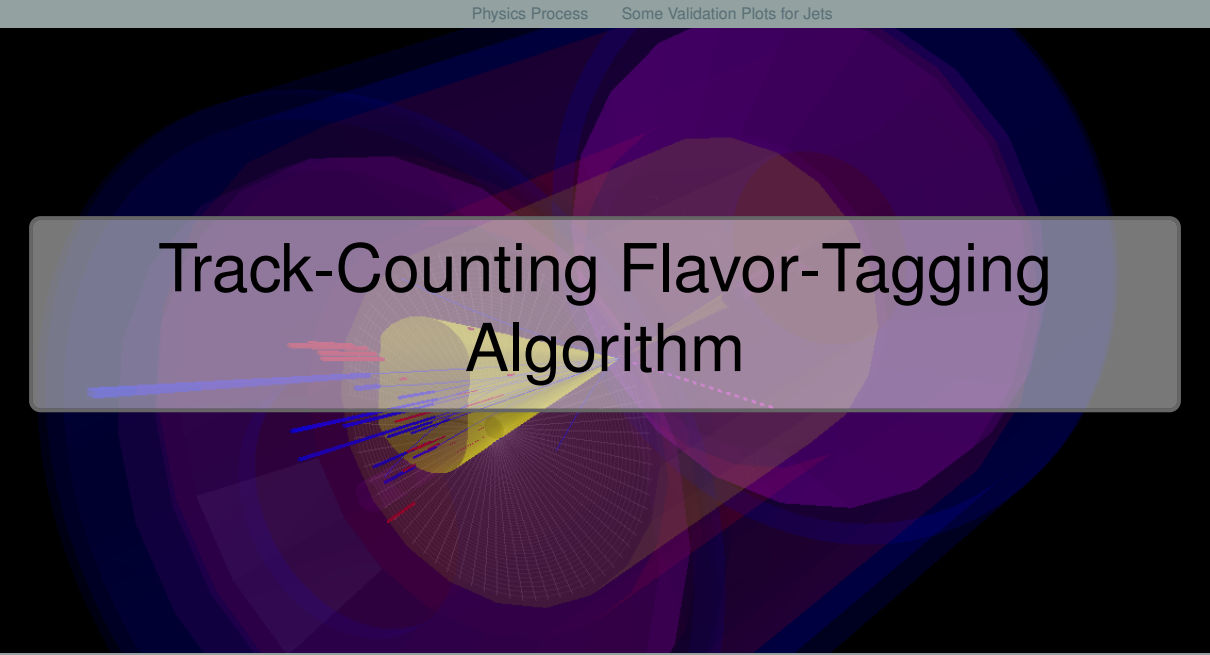

Track-Counting Flavor-Tagging Algorithm

Flavor Tagging by Track Counting

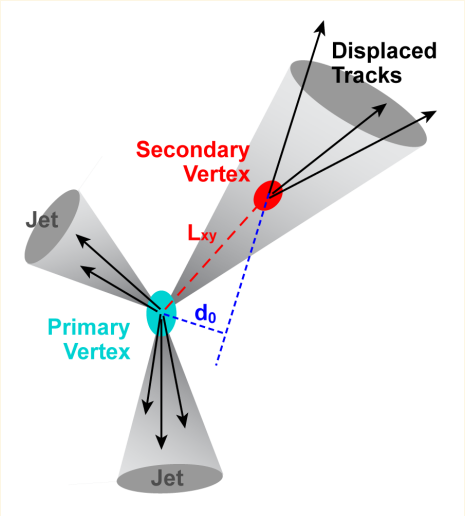

Graphic from ATLAS b-jet Trigger Signature Group

Delphes provides a nice, basic flavor tagging algorithm: high-impact-parameter track counting inside a jet object.

- Track $p_T^{min} = 1\ \mathrm{GeV}$
- Track $IP^{max} = 3.0\,\mathrm{mm}$ (estimated using $\sim 2\times$ the expected charm meson flight length in a $p_T = 40\ \mathrm{GeV}$ jet, assuming the hadron carries half the jet energy)
- Use the 3-D signed impact parameter significance, and require $\mathrm{sIP_{3D}} > 2.2$ to count a track as "high-impact-parameter."
- Require ≥ 3 such tracks ("tight" setting).

See Appendix (slide 33) for existing validation of flavor tagging performance in Delphes against a real experiment (CMS). The "tightest" ("loosest") settings in modern jet charm-tagging algorithms (e.g. ATLAS or CMS) achieve 20% (40%) charm jet efficiency while accepting 0.5% (5%) of light jets.

Signed 3-D Track Impact Parameter (sIP_{3D})

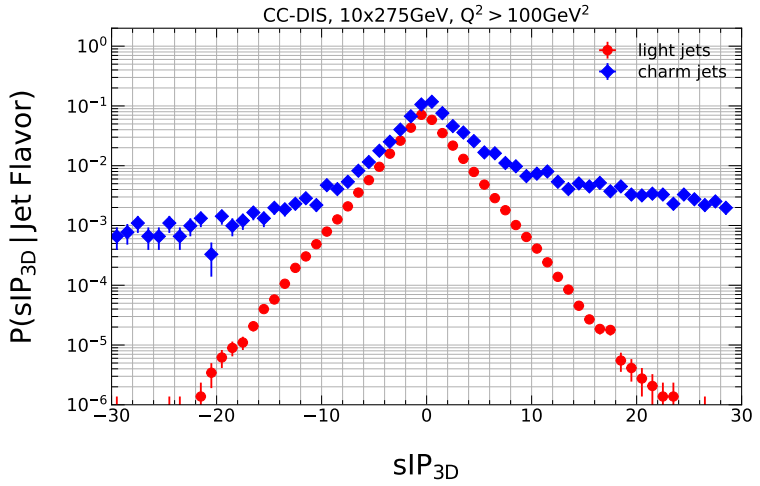

Example: Event Display of Charm Jet, 8 high-IP tracks, $E_T^{miss} = 24.7$ GeV, $p_T = 24.5$ GeV, $\eta = 1.6$

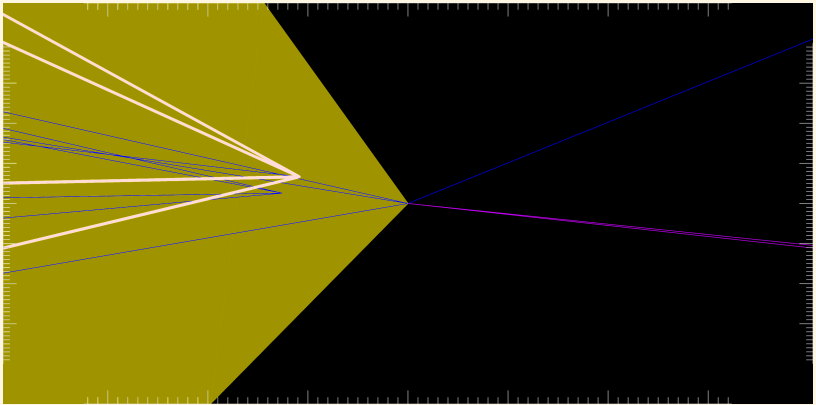

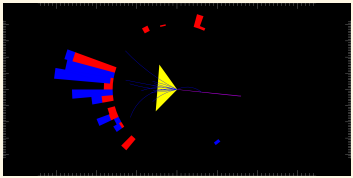

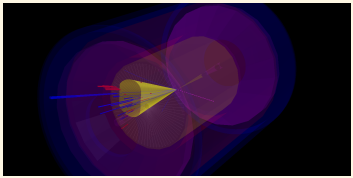

The displaced vertices in this jet (there are 2; 1 is highlighted) are about 0.5mm from the IP in $x - y$ plane. The jet was truth-matched to a charm jet and charm-tagged. Two true kaons are present, one emerging from each displaced vertex. Good case for jet-level tagging but also inclusion of PID in an inclusive tagging algorithm.

Flavor Tagging Efficiency

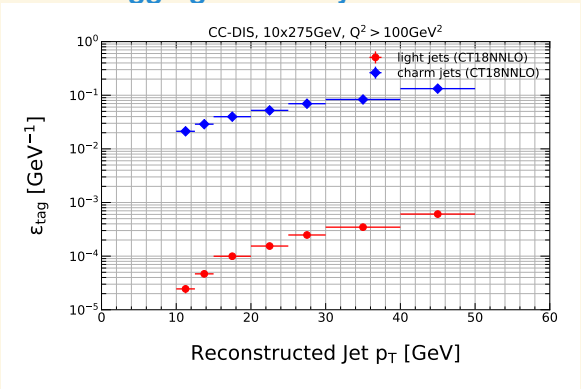

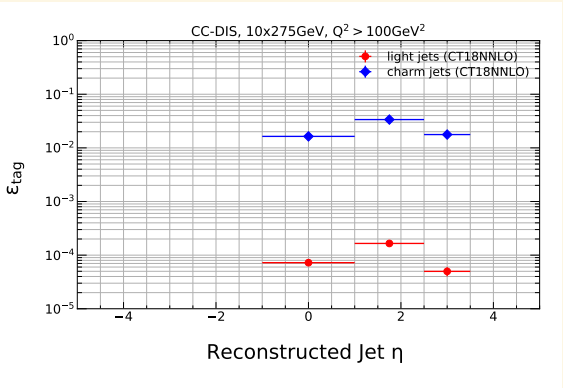

Track counting efficiency on charm jets ranges from 2-13%, while on light jets it's at the level of $10^{-5} - 10^{-3}$. As expected, tagging efficiency improves with jet p_T and discrimination weakens with increasing η (declining tracking efficiency).

Tagged Charm Jet Yields in 100fb^{-1}

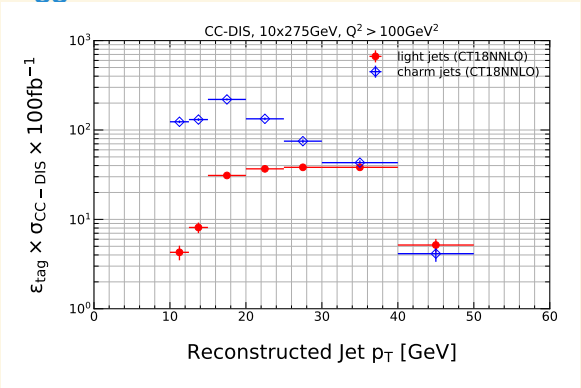

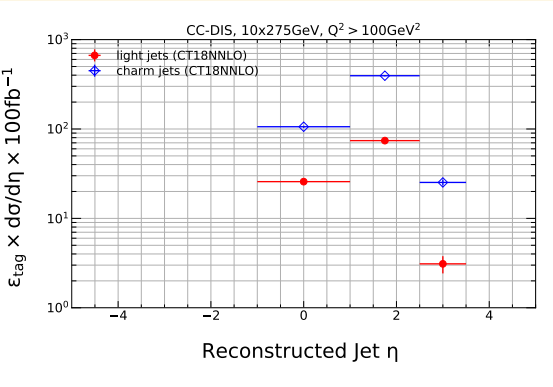

Even folding in a conservative tagging efficiency, expect $\mathcal{O}(1000)$ charm jets for study in 100fb^{-1}. Lots of room to improve here. Charm-to-light jet ratio in CC DIS looks promising.

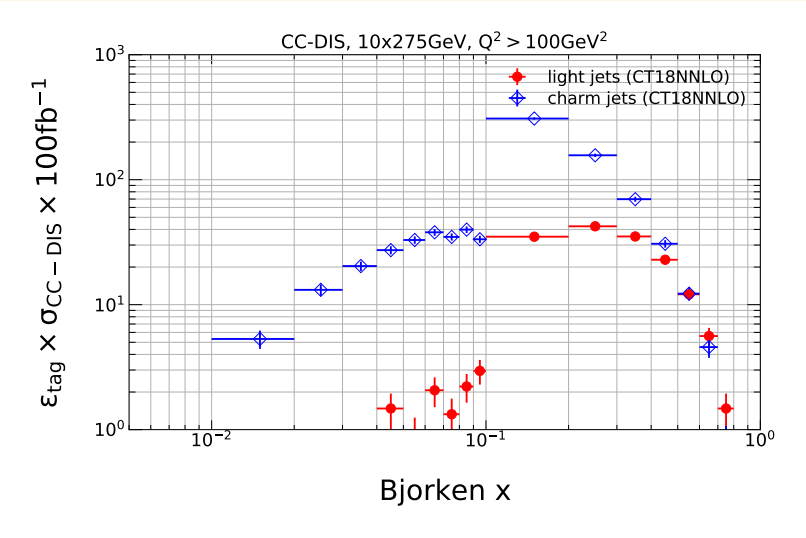

It is interesting to see where in x the charm yields distribute - from this simulation, the majority of candidates will be at $x > 0.1$.

Track Counting Flavor Tagging - Varying Parameters

Jets in this study are matched to either charm or light jets and have $p_T > 15$ GeV. The efficiency quoted is measured above the jet p_T threshold. In general, efficiency increases with p_T.

$min(p_T^{trk})$, $max(\lvert d_0 \rvert)$, $min(d_0/\sigma_{d_0})$	Tagging Efficiency (%) charm	light
1.0 GeV, 3 mm, 2.0	5.51 ± 0.16	0.059 ± 0.002
1.0 GeV, 3 mm, 2.2	4.90 ± 0.15	0.018 ± 0.001
1.0 GeV, 3 mm, 2.5	3.92 ± 0.14	0.002 ± 0.000
1.0 GeV, 6 mm, 2.0	5.65 ± 0.16	0.058 ± 0.002
0.5 GeV, 6 mm, 2.0	8.20 ± 0.19	0.099 ± 0.003
0.5 GeV, 3 mm, 2.0	8.38 ± 0.19	0.098 ± 0.003

Tagged Yields with Tighter $\mathrm{sIP_{3D}}$ Requirement

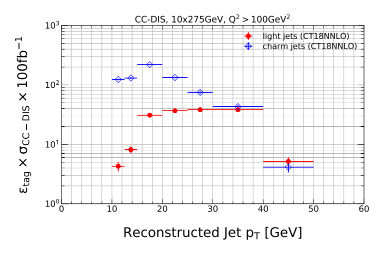

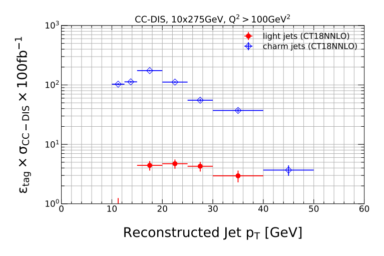

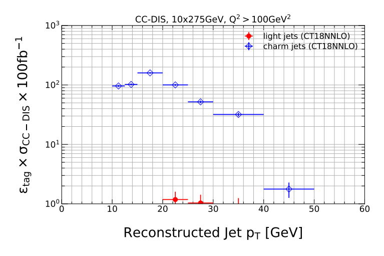

$\mathrm{sIP_{3D}} > 2.2$ $\mathrm{sIP_{3D}} > 2.5$ $\mathrm{sIP_{3D}} > 2.7$

Even slight adjustments to the $\mathrm{sIP_{3D}}$ threshold radically alters the charm-to-light ratio. For example, tightening this cut from $> 2.2 \rightarrow 2.7$ effectively removes all light jet contamination in this channel, while leaving about 70% of the charm jets.

Probing Strangeness in the Proton

SLIDE FROM TIM HOBBS[14]

nucleon strangeness remains comparatively less constrained

→ in CT, main inputs are from νDIS on heavy nuclei (nuclear corrs. relevant)

→ of interest: the strange suppression ratio, $R_s = \dfrac{s+\bar{s}}{\bar{u}+\bar{d}}$

→ typical QCD fits find $R_s \sim 0.5$; ATLAS W/Z production favors $R_s \sim 1$

→ ***question*: can CC charm jet production off <u>proton</u> distinguish small from large R_s?**

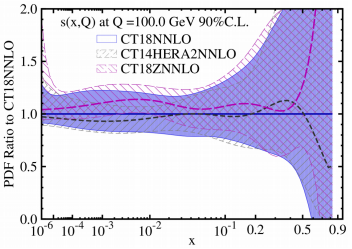

- Lagrange multiplier scans of R_s in CT18 analysis: arXiv: 1912.10053 [hep-ph]

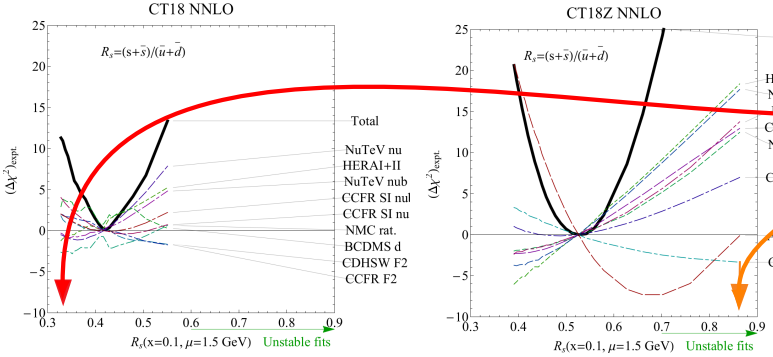

<u>theory inputs:</u> for

$x = 0.1,\ \mu = 1.5\,\mathrm{GeV}$

* $R_s = 0.325$ (CT18)

* $R_s = 0.863$ (CT18Z)

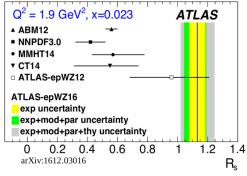

Statistical Uncertainty ($100\,\mathrm{fb}^{-1}$) vs. current theory uncertainty on Strangeness in the Proton

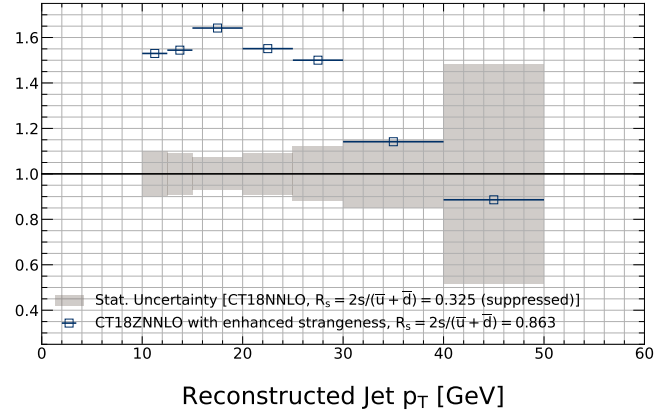

Tim Hobbs provided two variations of the CT18 PDFs: CT18NNLO with suppressed strangeness ($R_s = \frac{2s}{\overline{u}+\overline{d}} = 0.325$) and CT18ZNNLO with enhanced strangeness ($R_s = 0.863$). We compare the expected statistical error on a charm-tagged and reconstructed jet yield in $100\,\mathrm{fb}^{-1}$ with the range of variation in the predicted yields between the enhanced and suppressed strangeness cases.

We are very excited by the possibility that this channel will provide new inputs to the PDFs, even considering obvious systematics like jet energy scale ($\sim 10\%$), selection and trigger efficiencies and systematics, and the fact that we think this charm tagging efficiency is conservatively underestimated.

Strangeness Helicity: Potential Sensitivity ($100\,\mathrm{fb}^{-1}$)

DIS provides insight into $\Delta q + \Delta\bar{q}$. The $e^- p^+$ interactions discussed here give insight into $\Delta\bar{s}$, anti-strange quark helicity in the proton. These would be complementary to the insights from SIDIS and could be part of an eventual global analysis.

The uncertainty on the strangeness helicity measurement [15] will go roughly as

$$\delta A_i \approx \frac{1}{\sqrt{N_i(1+P_e)/2P_p}}$$

where P_p and P_e are the polarizations of the electron and proton beam (here, $P = 70\%$ is assumed for each), and i labels a bin.

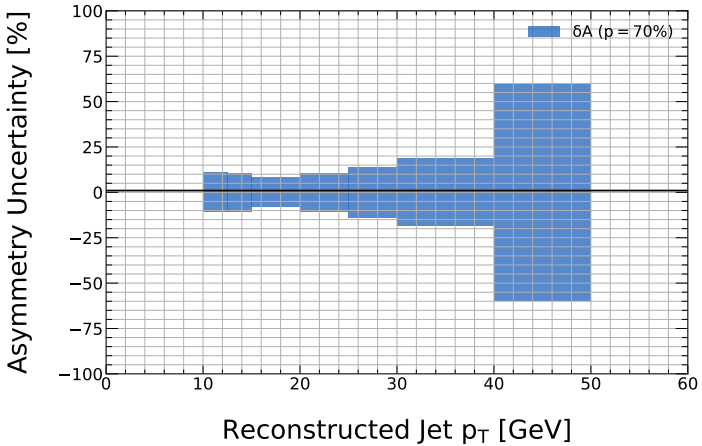

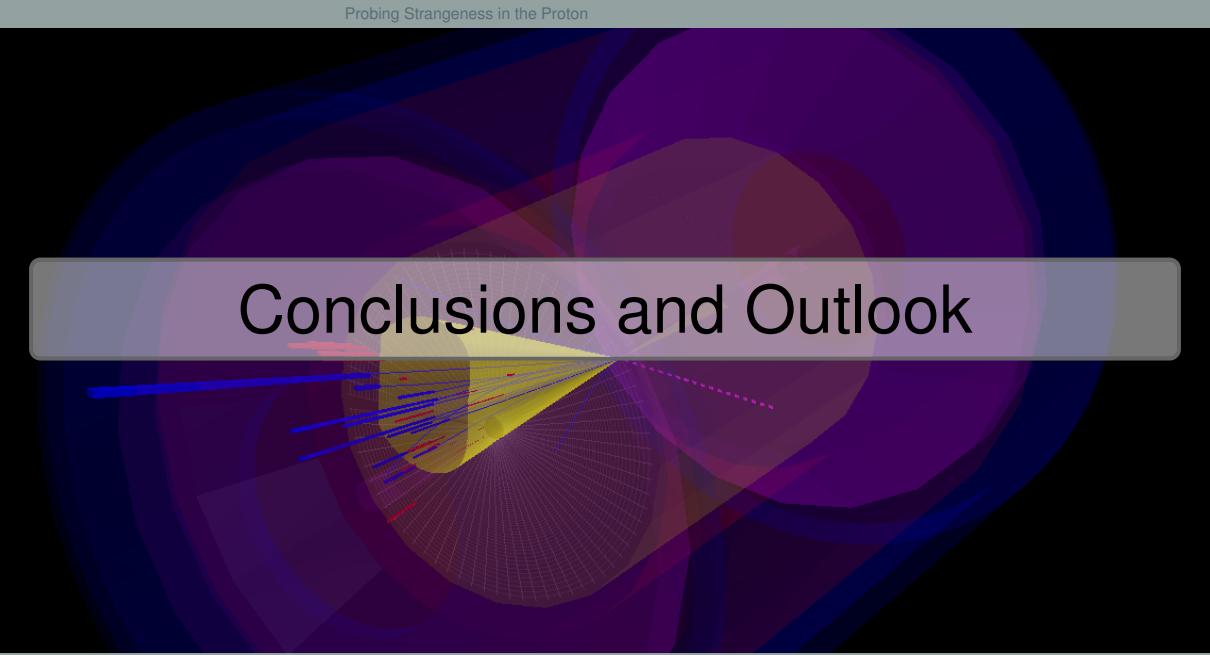

Conclusions and Outlook

Conclusions and Outlook

- We have an implementation of a baseline EIC-like detector in Delphes. The quick turnaround of this fast simulation allows us to rapidly engage in physics investigations (PDF variations, detector variations, etc.)
- We've explored charm jet production using an 10×275 EIC configuration; PDF set is CT18, PYTHIA8 is used to generate CC DIS events.
- We've reconstructed charm jets using high-impact-parameter track counting in R=1.0 jets.
- We are encouraged by the prospect for improving on our understanding of proton strangeness using charm jets.
- Charm jets from EIC collisions look to be a promising playground/physics benchmark for understanding decision impacts.
- One of the kinematic coverage plots requested by the Jets/HF Conveners is in the Appendix, slide 35.

Future Directions

- HCal configuration variations
- Tracking and vertexing resolution (more realistic vertex resolution model)
- Particle ID (efficiency, separation)
- B-field choice (1.5T or 3.0T)
- Implement a more advanced charm tagger (e.g. using lessons from the many experiments in the last 20 years, especially) $\rightarrow$ observe how detector variations influence a more robust algorithm

Appendix

Approaches and Challenges

Channels listed are increasingly demanding. For every row consider all requirements above as well. The (x, Q^2) dependence of the observables is omitted for brevity. Table from Miguel Arratia.

Channel	Observable	Goal	Physics-driven requirement	Category	numbers
e-jet (NC) 100 fb^{-1}	$d\sigma$, $A_{UT}(\Delta\phi)$	k_T-dependence of quark Sivers	$\Delta\phi$ res. $<<$ intrinsic width $R = 1.0 \rightarrow$ had. corr. $O(1)$% particle-flow reco	Jet res. Acceptance Granularity	jet $dE/E < 15$% 2π, $\lvert\eta\rvert < 3.5$ HCAL and ECAL endcap $\Delta\phi \times \Delta\eta \leq 0.025 \times 0.025$
h-in-jet (NC) 100 fb^{-1}	$d\sigma$, $A_{UT}(z_h, j_T)$	q-transversity	$+$ dp/p at high $z <$ jet dE/E	Tracker PID	$dp/p < 5$% at 50 GeV $\eta < 3.5$ and 40 GeV
ν-jet (CC) 100 fb^{-1}	$d\sigma$, A_{UT}	u Sivers	$\Delta\phi <<$ 0.3 rad Bkg. rej. to phot and NC $>$70% survival prob. for 5 bins per-decade in x, Q^2	E_T^{miss} res. Acceptance Jet/E_T^{miss} res.	$dE_T^{miss}/E_T^{miss} < 15$% 2π, $\lvert\eta\rvert < 3.5$ HCAL and ECAL E$>$100 MeV thres. ECAL E$>$400 MeV thres. HCAL $p_T > 100$ MeV tracker $dx/x < 20$%, $dE_T^{miss}/E_T^{miss} < 15$%
h-in-jet (CC) 100 fb^{-1}	$d\sigma$, $A_{UT}(z_h, j_T)$	u-transversity	—	—	—
c-jet (CC) 100 fb^{-1}	$d\sigma$, A_{LL}	s PDF& helicity	charm-tagging	Tracker PID	c-jet tag at $>$ 10% ($<$0.05%) DCA = 20 μm, $\approx$ 100% eff. TBD
h-in-c-jet (CC) 100 fb^{-1}	$d\sigma$, $A_{UT}(z_h, j_T)$	s-transversity	—	—	—
c-jet (e^+ CC) 100 fb^{-1}	$d\sigma$, A_{LL}	$s/\bar{s}$ asymmetry	positrons	—	—

CC DIS NLO Cross-Section Prediction

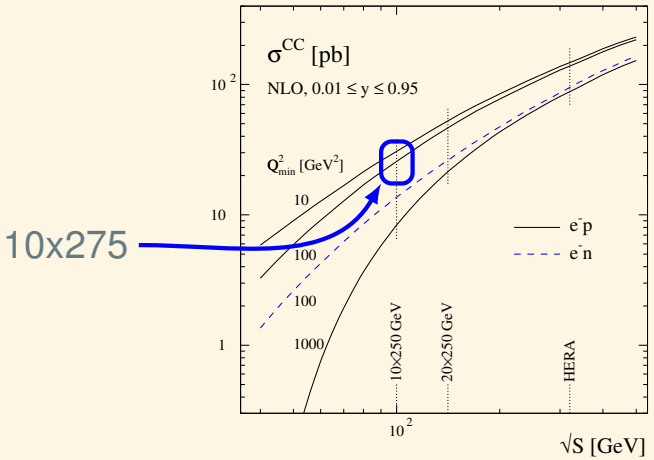

Total CC DIS rate at EIC with 10x275 configuration ($\sqrt{s} = 105$ GeV) is about 20pb.

Figure is from Ref. [16].

Background Charm Jet Production at the EIC

The CC DIS process $W^- \bar{s} \to \bar{c}$ is, of course, not the only contributor to charm jet production at an electron-hadron machine [17].

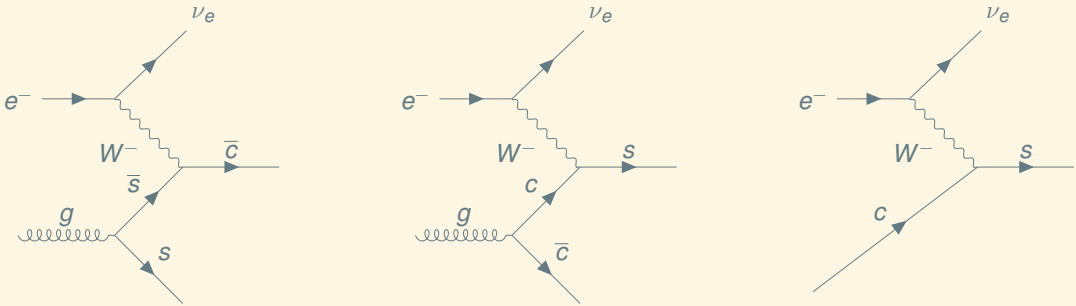

Charm jets can be produced by Wg fusion (left and center diagrams), and so can probe the gluon splitting inside the proton; they can also be produced by intrinsic charm in the proton, which can result in a scattered remnant jet from the proton that contains heavy flavor. These components need to be disentangled in a full-scale data analysis.

Delphes and Detector Implementation[6]

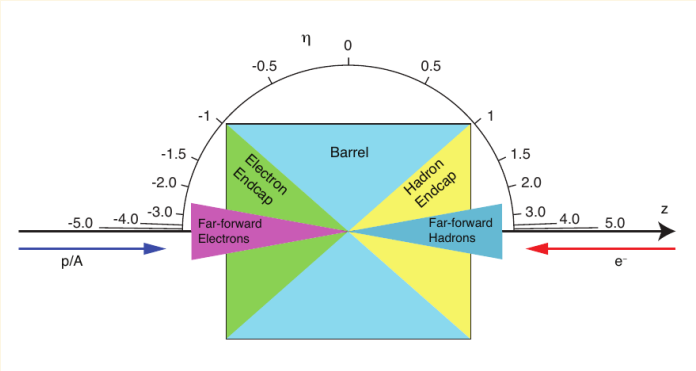

Charged particle tracking covers $|\eta| < 3.5$ and is efficient for tracks with $p_T > 0.1\mathrm{GeV}$. **For this study, the track d_0 and z_0 resolution formulas are each set to $20\mu\mathrm{m}$ for all (p_T, η) where this tracker model has acceptance.**

- Implementation in Delphes by Miguel[7] based on EIC Detector Matrix [9]; a fork is used for studies in this talk [8]
- Consists of a tracking system, ECal, and HCal. Tracker is immersed in 1.5T solenoidal magnetic field.

Tracker Information

- For particles below 0.1 GeV in p_T, or with $|\eta| > 3.5$, efficiency is 0.
- For particles with $p_T = (0.1, 1.0]$, efficiency varies from 95% for $|\eta| \leq 1.5$, to 92% for $|\eta| = (1.5, 2.5]$, to 85% for $|\eta| = (2.5, 3.5]$.
- For particles with $p_T > 1.0$, efficiency varies from 98% for $|\eta| \leq 1.5$, to 95% for $|\eta| = (1.5, 2.5]$, to 90% for $|\eta| = (2.5, 3.5]$.

Delphes and Detector Implementation[6]

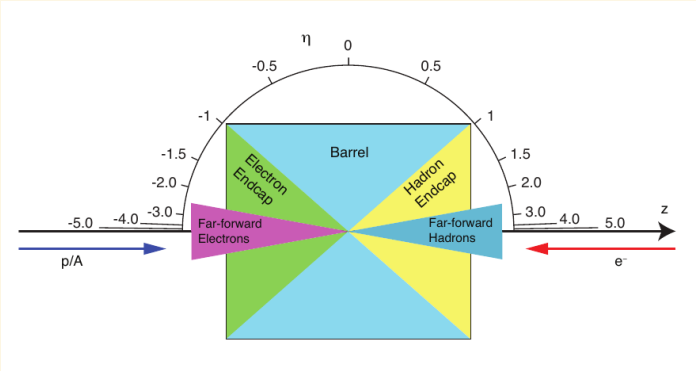

The barrel and endcap electromagnetic calorimeters ($|\eta| < 1.0$ and $|\eta| = [1.0, 4.0]$, respectively) are assumed to have a granularity of $(\Delta\eta, \Delta\phi) = (0.020, 0.020)$. The minimum cell energy threshold is set to 0.2 GeV.

- Implementation in Delphes by Miguel[7] based on EIC Detector Matrix [9]; a fork is used for studies in this talk [8]
- Consists of a tracking system, ECal, and HCal. Tracker is immersed in 1.5T solenoidal magnetic field.

ECal Information

- For $|\eta| = (-4.0, -2.0]$, $\sigma^2 = E^2 \times (1.0\%)^2 + E \times (2.0\%)^2$
- For $|\eta| = (-2.0, -1.0]$, $\sigma^2 = E^2 \times (1.0\%)^2 + E \times (7.0\%)^2$
- For $|\eta| = (-1.0, 1.0]$, $\sigma^2 = E^2 \times (1.0\%)^2 + E \times (10.0\%)^2$
- For $|\eta| = (1.0, 4.0]$, $\sigma^2 = E^2 \times (2.0\%)^2 + E \times (12.0\%)^2$

Delphes and Detector Implementation[6]

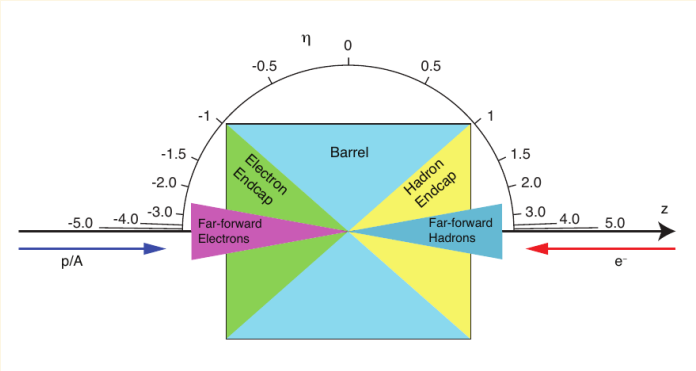

The EIC baseline detector does not describe the granularity of an HCal. (an $\approx$ sPHENIX HCal is assumed). The barrel hadronic calorimeter ($|\eta| < 1.0$) has $(\Delta\eta, \Delta\phi) = (0.1, 0.1)$; the endcap ($|\eta| = [1.0, 4.0]$) has $(\Delta\eta, \Delta\phi) = (0.025, 0.025)$, improved over barrel. Resolution also improves in the endcap. The minimum cell object threshold is set to 0.4 GeV.

- Implementation in Delphes by Miguel[7] based on EIC Detector Matrix [9]; a fork is used for studies in this talk [8]
- Consists of a tracking system, ECal, and HCal. Tracker is immersed in 1.5T solenoidal magnetic field.

HCal Information

- For $|\eta| = (-4.0, -1.0]$, $\sigma^2 = E^2 \times (10.0\%)^2 + E \times (50.0\%)^2$
- For $|\eta| = (-1.0, 1.0]$, $\sigma^2 = E^2 \times (10.0\%)^2 + E \times (100.0\%)^2$
- For $|\eta| = (1.0, 4.0]$, $\sigma^2 = E^2 \times (10.0\%)^2 + E \times (50.0\%)^2$

Validation Plots for Reconstructed Jets (R=1.0)

Jets are reconstructed using tracks and calorimeter clusters in an EnergyFlow approach. The Anti-k_T algorithm builds the jet (R=1.0) and energy flow is used to determine the jet four-vector. The reconstruction implementation comes from FastJet [12, 13].

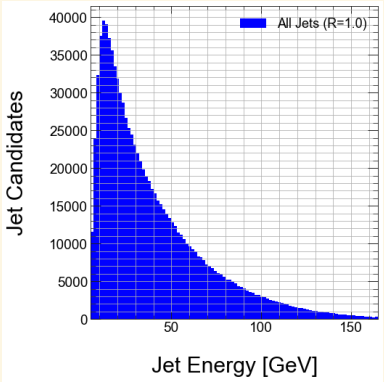

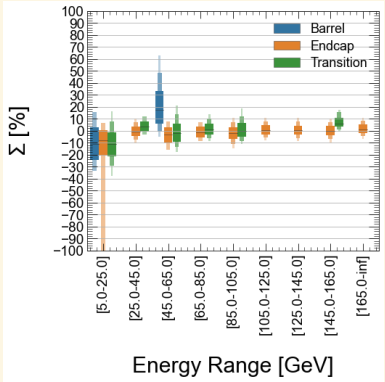

Jet energy resolution ($\Sigma \equiv (E_J - E_J^{true})/E_J^{true}$) in this detector model varies with jet energy, of course, but generally has an RMS that varies between 15-20% at low E_J to 5-10% at higher E_J.

Barrel jet resolution is worse than endcap resolution ($\sim$ 20% vs. $7.5 - 15\%$).

The "Transition" region is the one between the barrel and endcap(s). I set that to be between $|\eta| = [0.5, 1.5]$ given the size of the jets.

True jets are matched to reconstructed jets if they fall within half the radius parameter of the reconstructed jet axis. Closest in $\Delta R = \sqrt{(\Delta\phi)^2 + (\Delta\eta)^2}$ is retained.

Example: Delphes vs. CMS

Performance : High Purity

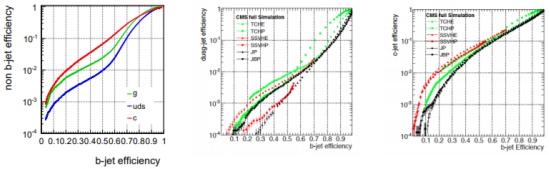

- c mistag rate agrees ok
- too pessimistic light rejection for low btagging efficiency

At 55% b-tagging efficiency (Medium working point) :

DELPHES : l-mis = 1.5%, c-mis = 10%
CMS : l-mis = 1.0%, c-mis = 10%

$sig(IP)_{min} = 6.5$

Slide from Ref. [18]

Dedicated charm-jet taggers developed for LHC experiments (e.g. ATLAS) use multivariate discriminants that combine 2-D and 3-D track impact parameter information with secondary vertex and jet evolution information. In their loose (tight) configurations they can select 40% (20%) of charm jets while keeping only 25% (5%) of b-jets and 5% (0.5%) of light jets. That's "state-of-the-art" for now.

Standard EIC Plots for Kinematic Coverage - Generator-Level Jet Momentum

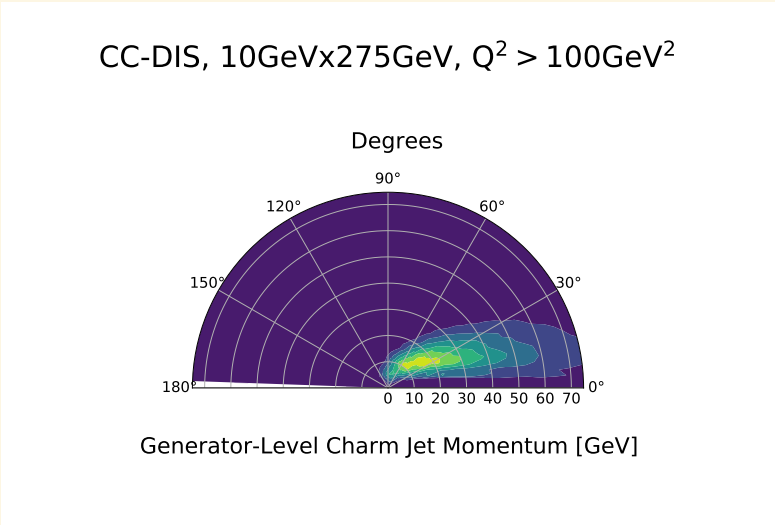

Standard EIC Plots for Kinematic Coverage - Jet Momentum

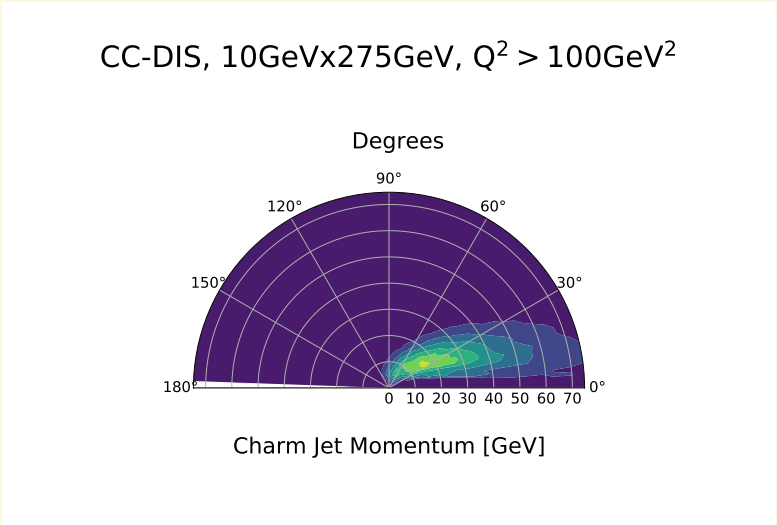

References I

[1] "The EIC Machine." https://www.bnl.gov/eic/machine.php.

[2] E. C. Aschenauer, M. D. Baker, A. Bazilevsky, K. Boyle, S. Belomestnykh, I. Ben-Zvi, S. Brooks, C. Brutus, T. Burton, S. Fazio, A. Fedotov, D. Gassner, Y. Hao, Y. Jing, D. Kayran, A. Kiselev, M. A. C. Lamont, J. H. Lee, V. N. Litvinenko, C. Liu, T. Ludlam, G. Mahler, G. McIntyre, W. Meng, F. Meot, T. Miller, M. Minty, B. Parker, R. Petti, I. Pinayev, V. Ptitsyn, T. Roser, M. Stratmann, E. Sichtermann, J. Skaritka, O. Tchoubar, P. Thieberger, T. Toll, D. Trbojevic, N. Tsoupas, J. Tuozzolo, T. Ullrich, E. Wang, G. Wang, Q. Wu, W. Xu, and L. Zheng, "eRHIC Design Study: An Electron-Ion Collider at BNL," 2014.

[3] Ferdinand Willeke, "EIC accelerator and IR design status," in *2nd EIC Yellow Report Workshop at Pavia University*. 2020. https://indico.bnl.gov/event/8231/contributions/37060/.

[4] Leticia Cunqueiro and Brian Page and Frank Petriello and Ernst Sichtermann and Ivan Vitev, "Jets and Heavy Quark WG Summary," tech. rep., 2020. https://indico.bnl.gov/event/7449/contributions/35839/attachments/27288/41619/jhqSummary_v1.pdf.

[5] **H1** Collaboration, F. Aaron *et al.*, "Measurement of the Charm and Beauty Structure Functions using the H1 Vertex Detector at HERA," *Eur. Phys. J. C* **65** (2010) 89–109, arXiv:0907.2643 [hep-ex].

References II

[6] E. Aschenauer, A. Kiselev, R. Petti, T. Ullrich, C. Woody, P. Nadel-Turonski, L. Gonella, and P. Jones, "Electron-Ion Collider Detector Requirements and R&D Handbook," tech. rep., 2019.

[7] https://github.com/miguelignacio/delphes_EIC.

[8] https://github.com/stephensekula/delphes_EIC.

[9] "EIC Detector Matrix," 2020. https://physdiv.jlab.org/DetectorMatrix/.

[10] T. Sjöstrand, S. Mrenna, and P. Skands, "A brief introduction to pythia 8.1,"*Computer Physics Communications* **178** (Jun, 2008) 852867. http://dx.doi.org/10.1016/j.cpc.2008.01.036.

[11] T. Sjöstrand, S. Mrenna, and P. Skands, "Pythia 6.4 physics and manual,"*Journal of High Energy Physics* **2006** (May, 2006) 026026. http://dx.doi.org/10.1088/1126-6708/2006/05/026.

[12] M. Cacciari, G. P. Salam, and G. Soyez, "Fastjet user manual,"*The European Physical Journal C* **72** (Mar, 2012) . http://dx.doi.org/10.1140/epjc/s10052-012-1896-2.

[13] M. Cacciari and G. P. Salam, "Dispelling the n^3 myth for the k_t jet-finder,"*Physics Letters B* **641** (Sep, 2006) 5761. http://dx.doi.org/10.1016/j.physletb.2006.08.037.

References III

[14] Tim Hobbs, "Update ongoing PDF studies for EIC IRG," in *2nd EIC Yellow Report Workshop at Pavia University*. 2020. https://indico.bnl.gov/event/8231/contributions/37765/.

[15] S. Kretzer and M. Stratmann, "Next-to-Leading order QCD corrections to charged current charm production and the unpolarized and polarized strange sea at HERA," *The European Physical Journal C* **10** (Aug, 1999) 107119. http://dx.doi.org/10.1007/s100529900116.

[16] E. C. Aschenauer, T. Burton, M. Stratmann, T. Martini, and H. Spiesberger, "Prospects for charged current deep-inelastic scattering off polarized nucleons at a future electron-ion collider," *Physical Review D* **88** (Dec, 2013) . http://dx.doi.org/10.1103/PhysRevD.88.114025.

[17] **ZEUS** Collaboration, I. Abt *et al.*, "Charm production in charged current deep inelastic scattering at HERA," *JHEP* **05** (2019) 201, arXiv:1904.03261 [hep-ex].

[18] CP3 UCL, "Impact parameter b-tagging in DELPHES," 2104. https://cp3.irmp.ucl.ac.be/projects/delphes/raw-attachment/wiki/WorkBook/Modules/btagging_v2.pdf.